AIMS Bioengineering, 7(4): 224–235.
DOI: 10.3934/bioeng.2020019
Received: 27 April 2020
Accepted: 27 June 2020
Published: 15 July 2020

http://www.aimspress.com/journal/Bioengineering

Research article

Monte Carlo dose index estimation in computed tomography

Moncef ATI[1,*], Rachid BOUAMRANE[2], Djamel ADDI[3], Fatima Zohra MAROC[3] and Fatima Zohra Mecheret[3]

[1] Faculty of Medicine, University of Abdelhamid Ibn Badis, 27000 Mostaganem, Algeria
[2] LEPM, Faculty of Physics, University of Sciences and Technology of Oran MB, BP 1505 El M'Naouer, 31000 Oran, Algeria
[3] Faculty of Physics, University of Sciences and Technology of Oran MB, BP 1505 El M'Naouer, 31000 Oran, Algeria

*** Correspondence:** Email: moncef.ati@univ-mosta.dz.

Abstract: We numerically study the computed tomography dose index (CTDI) quantity based on the Monte Carlo method using GATE software. In this work, it was demonstrated that the CTDI values decreased following an exponential form as a function of phantom diameter. As expected, the absorbed dose is shown to have a good relationship which increases linearly with X-ray tube current (mAs) values. The simulation presented in particularly that the (CTDI) dose increases not-linearly dependence with photon deposited energy (kVp). It seems that the average percent of the absorbed dose in the abdominal phantom was lower than the heat phantom object's absorbed dose, which was equal to 80%. In conclusion, the use of Monte Carlo simulation represents a dosimetry tool for radiation protection in the field of radiology imaging.

Keywords: Monte Carlo; simulation; absorbed dose; CTDI; CT; dosimetry

1. Introduction

The ionization radiation devices are presently very common at the present time in different medical areas, being the most important tool in the diagnostics process. One of the applications of ionization radiation as X-ray computed tomography demand knowledge of the radiation energy deposited in the matter to estimate biological effects [1,2]. Where the computed tomography (CT) examination gives around 10–50 more doses than the absorbed doses to a patient under conventional X-ray radiology [3], in the other hand, the number of CT examinations has been rapidly increasing in

recent year, this is explained by the reason that the CT exam is more interpretable than the conventional radiology by the radiologists [4]. There is the problem of patient exposition over several problems of medical physics and radiation protection to be solved. In 2005 BEIR VII [5] and 103 ICRP [6] reports mentioned that the risk assessment depends on tow parameters: first, the patient organ dose. Second, it is patient sex. Here the organ's absorbed dose for different energy photons was larger than the lower energy photon (kVp) at the same current tube (mAs), because of their penetration power. However, the minimization of radiation absorbed doses is very suitable, where recently the development of modern technology research in CT scan devices based on the dynamic filter [7] plays a crucial role in the performance optimization techniques, by placing a dynamic Bowtie filter between the X-ray source and the patient to be imaged in the FOV region. In this case, the beam filtered by the dynamic Bowtie filter optimizes the beam intensity. The proposed technique of the dynamic Bowtie filter reduced the scattering beam by blocking the low energy of the X-ray source. One of the most important methods of estimating the absorbed dose on the medical imaging system has been involved in the Monte Carlo simulation code to calculate the absorbed dose into different organs [8,9,10,11]. This approach is based on random variable sampling, where it comes very usually into use in several advanced numerical simulation techniques such as generalized methods. However, radiation doses in conventional radiology examinations such as computed tomography (CT) examinations are often performed using GATE. The GATE (Geant Application for Tomography Emission) was created to simulate all kinds of interactions between matter and particles in the area of medical imaging and radiotherapy. Where the GATE is an important tool to obtain an estimated absorbed dose in radiology devices based on the stochastic process [12,13]. There are some studies based on GATE software using different X-ray spectrum production based on the SRS-78 program [14] was completed, also using Mote Carlo techniques [15]. Dosimetry in CT scan is an important aspect of conventional radiology to estimate the risk versus benefit factor [16].

2. Materials and methods

The CT dose index estimation was performed on a circular phantom made by PMMA (Polymethylmetacryhate). The phantom contains different cylindrical holes of diameter equal to 10 mm to put the detector inside the field of view (FOV) region. The geometry of the PMMA phantom was configured as illustrated in Figure 1. Hence, the Computed Tomography Dose Index (CTDI) estimating must be made regularly to ensure the CT performance. Gate/Geant4 model was used to build a computational model for estimation the deposited doses in the CT scan system, where different CT parameters (Slice, kVp, mAs) have been used to evaluate the dose index value with a 1 cm beam collimator by irradiating the cylindrical phantom with a fan-beam from an X-ray tube in a rotation motion [17,18]. Figure 1 shows the simulation set up used in the present work. Here we have the phantom and the scanner couch rotated around the z-axis, and the scanner couch was rotated around the z-axis, and the X-ray tube was in a stationary position as shown in Figure 1.

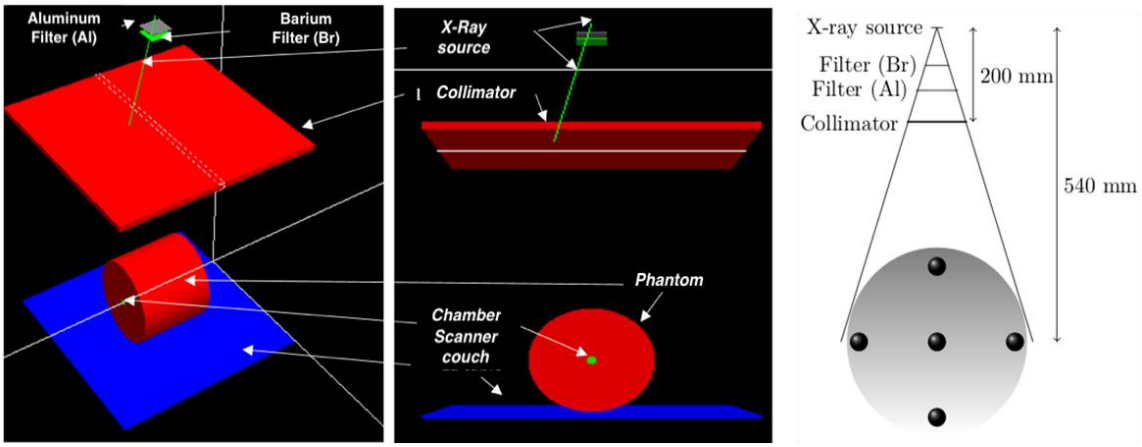

Figure 1. Various positions of the ionization chamber in the CTDI phantom around the z-axis.

The study was performed by Monte-Carlo simulation to evaluate the absorbed dose in CT procedures using Gate software. In witch, all computer tomography doses index (CTDI) measurements were performed on PMMA phantom (head and abdominal) with the length of 15 cm and the diameter between 16 and 32 cm, respectively, the PMMA phantom was positioned at a distance equal to 54 cm from the X-ray source to the PMMA iso-center, according to the manufacturer's protocols. The measurements were analyzed under several-tube current range between 100–450 (mAs) in five regions of the PMMA phantom in the central hole position ($CTDI_c$), and at four peripheral holes ($CTDI_p$) (see Figure 1) using a pencil ion chamber positioned at the different holes of the PMMA phantom covered by a polyacetal cap which had an active volume of 2.9 cm^3 and a length equal to 10 cm [19], after that the mean values were used to calculate the relative dose width profile in the irradiated ($CTDI_w$) volume according to the Eqs 1 and 2. The X-ray photon energy spectra were performed between 40–140 kVp using SPEKTR3.0 software based on the TASMICS algorithm [20], applied a slice filter equal to 5.21 mm of Barium and 1.32 mm of Aluminum, this filter was mounted on the gantry to reduce the scattering and inhomogeneous photons of the con-beam after passing through a Bowtie filter, filters are shown in Figure 1. The X-ray con-beam was adjusted using a collimator of 1 cm tungsten thickness. In each run, 10^7 particles have been generated. In particular, scan imaging time is equal to 1-sec rotation (acquisition time). The computed tomography dose index along the z-axis is calculated according to the Eq 1:

$$CTDI_{100} = \frac{1}{B.W}\int_{-\frac{L}{2}}^{+\frac{L}{2}} D\,(z).\partial z \tag{1}$$

where:

$D(z)$ represents the dose profile along the rotation axis z.

B.W is the X-ray beam width.

z is the width profil.

L ionization chamber length.

The dose length $CTDI_w$ is given by the following the Eq 2:

$$CTDI_w = \frac{1}{3}CTDI_{100,c} + \frac{2}{3}CTDI_{100,p} \tag{2}$$

When the CTDI quantity was calculated in terms of the integral over the length of phantom, from $-\frac{L}{2}\ to\ +\frac{L}{2}$ following the equation 1 [21].

3. Results

3.1. Spectral measurements

Simulates X-ray spectra using SPEKTR3.0 software [19], several variables that impact the X-ray beam spectrum are defined as anode angle, filter thickness, and material. SPEKTR3.0 is a computational toolkit that calculates X-ray spectra using TASMICS algorithm spectral model [22]. The SPEKTR3.0 toolkit includes a Matlab release 2013b (The Mathworks, Natick MA) to calculate X-ray beam spectra. Figure 2 shows the X-ray beam profile calculated using various photon energy (kVp) and tube current (mAs) variables.

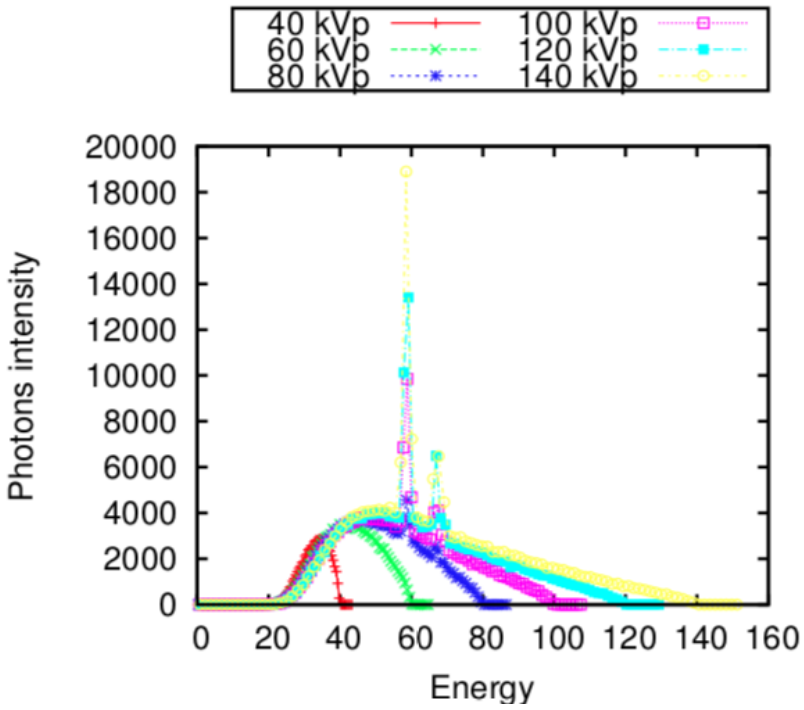

Figure 2. The different X-ray beam spectra obtained using SPEKTR3.0 software.

The dependences of $CTDI_{100,c}$, $CTDI_{100,p}$ and $CTDI_{100,w}$ on the photon energy (kVp) under various tube current (mAs) are shown in Figures 3–5, respectively. The X-ray beam thickness was equal to 1 cm. For the same parameters, the dependencies of absorbed dose (CTDI) on the PMMA phantom diameter under several (kVp) and (mAs) of photon beams are shown in Figures 6 and 7. Figures 8 and 9 show that the CTDI at the iso-center of the central hole is a function of tube current (mAs) for several PMMA phantom diameter and photon energy (kVp), respectively. A fit represented by a dashed line is shown in Figure 10 calculation processes in this study, that $CTDI_{100,w}$ was calculated using 140 kV and 1 sec acquisition time for one rotation X-ray tube.

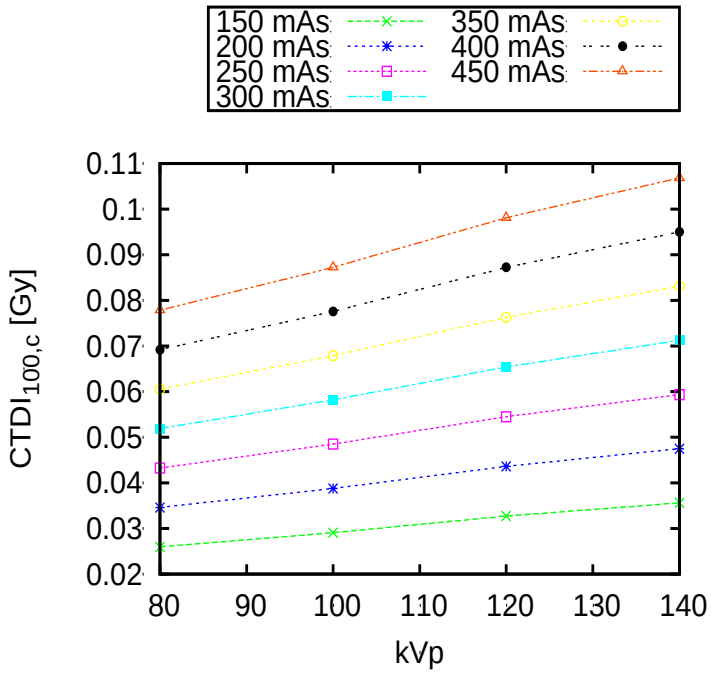

Figure 3. $CTDI_{100,c}$ for the central hole as function kVp, 1 sec and 1 cm slice thickness under various mAs.

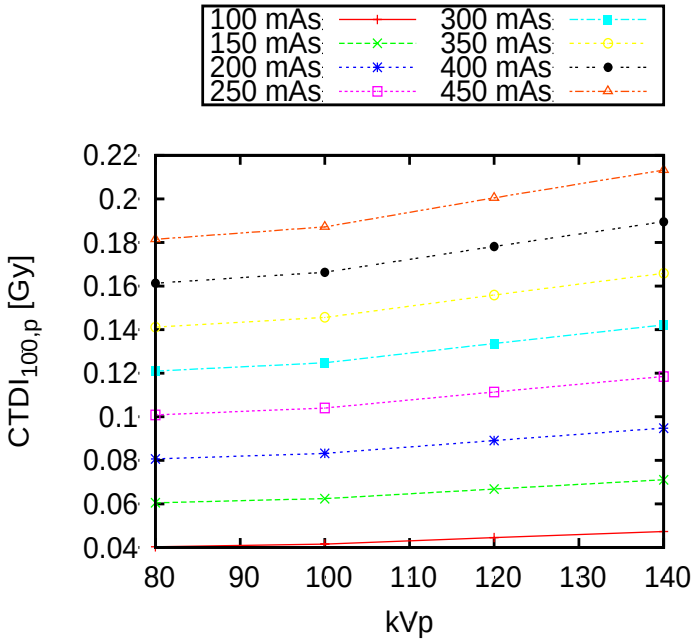

Figure 4. $CTDI_{100,p}$ for the peripheral holes as function kVp, 1 sec and 1 cm slice thickness under various mAs.

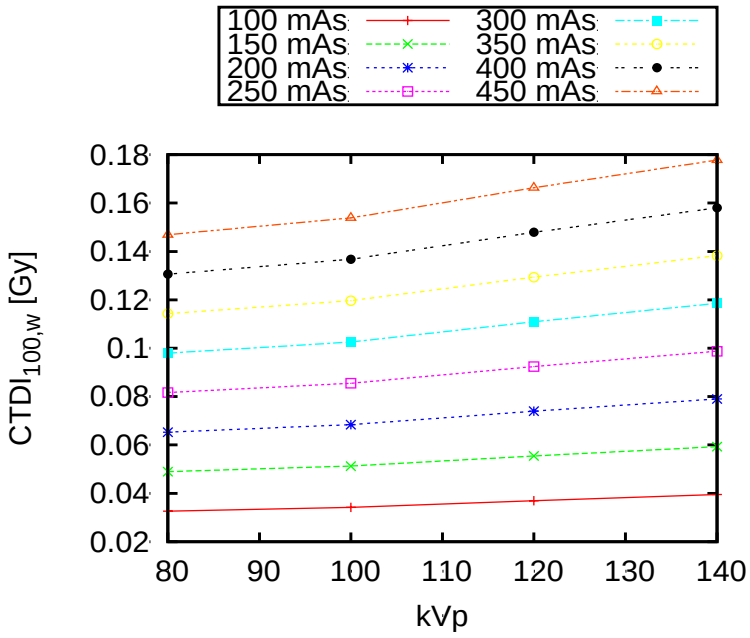

Figure 5. $CTDI_{100,w}$ as function kVp, 1 sec and 1 cm slice thickness under various mAs.

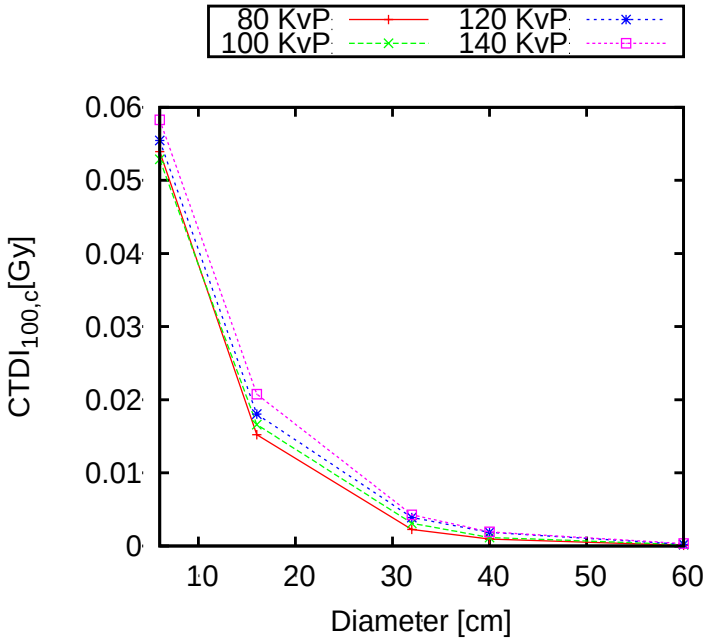

Figure 6. $CTDI_{100}$ of the central hole as function of diameter, mAs 100, 1 sec and 1 cm slice thickness for various kVp.

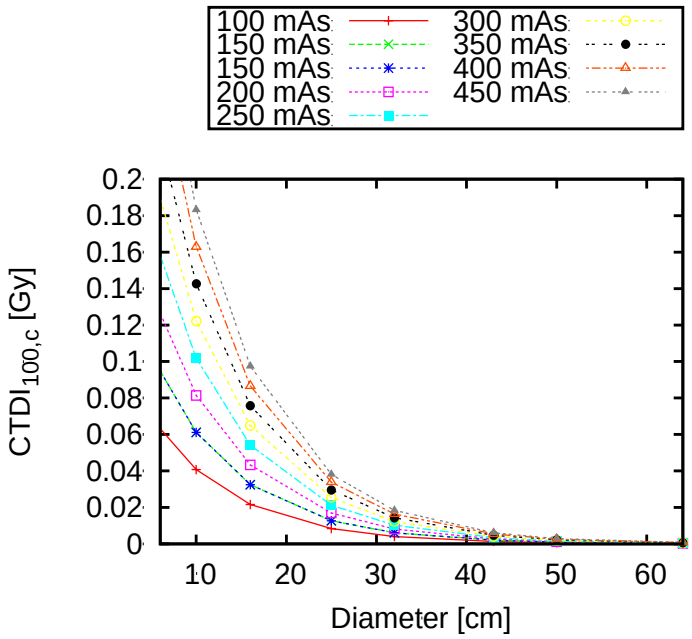

Figure 7. $CTDI_{100}$ of the central hole as function of diameter, 120 kVp, 1 sec and 1 cm slice thickness for various mAs values (100, 150, 200, 250, 300, 350, 400, 450).

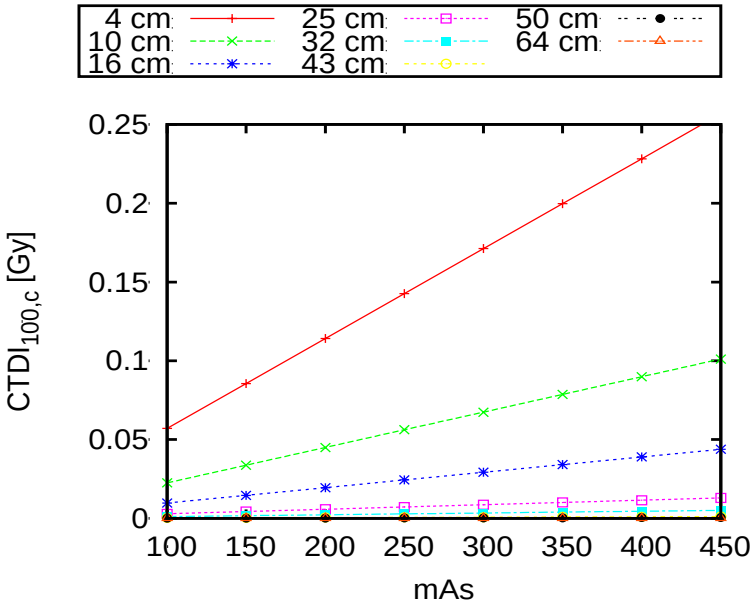

Figure 8. $CTDI_{100,c}$ of the central hole as function mAs, 120 kVp, 1 sec and 1 cm slice thickness for various diameters (4, 10, 16, 25, 32, 43, 50, 64).

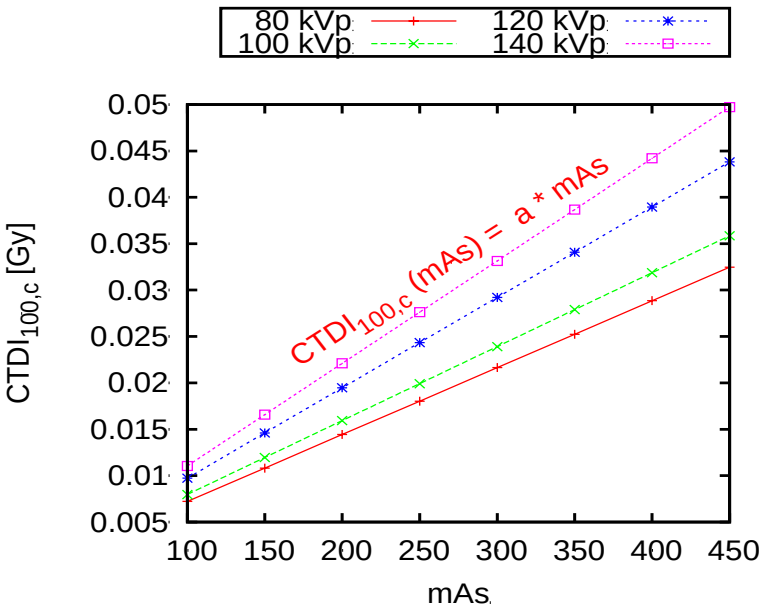

Figure 9. $CTDI_{100,c}$ as function of mAs, 1 sec and 1 cm slice thickness for various kVp (80, 100, 120, 140).

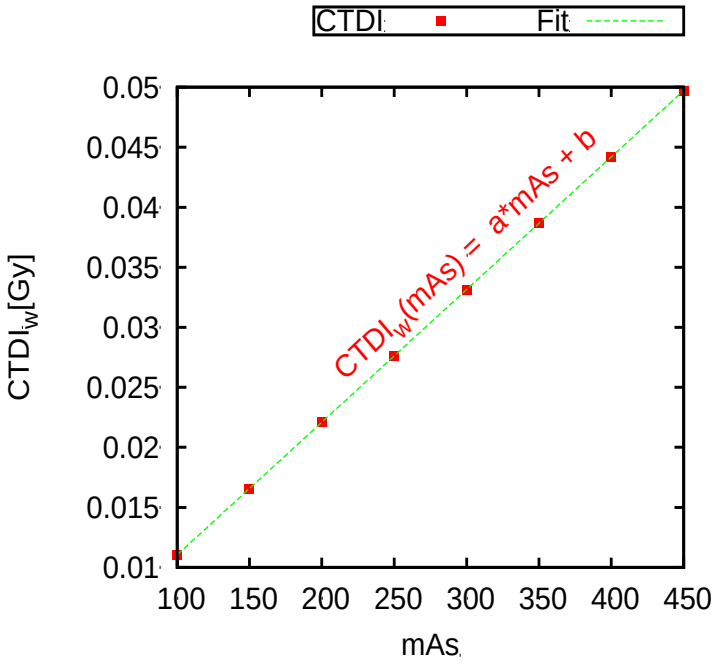

Figure 10. A linear fit of the $CTDI_w$ for 140 kVp as a function of tube current levels (mAs).

Table 1. CTDI (mGy) values for abdominal and head phantoms obtained under different photon energy (kVp), 100 mAs, 1 sec imaging time, and 1 cm collimation thickness.

kVp	Abdominal phantom	Head phantom
80	2.3	17.0
100	3.1	19.0
120	4.0	21.6
140	4.3	23.3

4. Discussion

According to Figures 3–5, the dose measurements of $CTDI_{100,c}$, $CTDI_{100,p}$ and $CTDI_{100,w}$ at the different points of the PMMA phantom (center and peripheral hole) under various current tube (mAs) was increased under a non-linearly way for several tube current values (mAs), already confirmed by the previous paper [15].

4.1. The behavior of CTDI values as a function of PMMA diameter

In these studies, the PMMA dose level was estimated for several diameters. Whereas, the results of these calculations are shown in Figures 6 and 7. For instance, the dose at the iso-center of the central hole ($CTDI_{100,c}$) for various kVp and mAs, respectively. Where it may be noted that the absorbed dose decreased non-linear when the PMMA diameter increases. Where the dose changed in an exponential way as a function of PMMA diameter. This is also the case for the abdominal PMMA phantom, in which the results for both phantoms confirm that the desired dose (CTDI) follows a relationship as a function of PMMA volume diameter for all photon energy values, according to the following equation:

$$\mathrm{CTDI(d)} = \mathrm{a} \times \mathrm{e}^{-\mathrm{b} \times \mathrm{d}} \tag{3}$$

where d represents the diameter of the CTDI phantom used.

In Figures 8 and 9, however, with increasing tube current (mAs), the measured CTDI values at the central position of the ionization chamber increase under a linear function way for each PMMA diameter and different X-ray beam energy (kVp) values, respectively. Contrary to the evolution of CTDI as a function of the photon energy (kVp) parameter where the dose increases, a non-linear shape was noted in Figure 3 at the same Monte Carlo simulation conditions.

In Figure 10, we have traced photon energy equal to 140 kV as a function of the current tube levels. This curve shows a linear increase by increasing the (mAs) values. To calculate the value for large (mAs) values, we perform a linear fit of the obtained points, the following equation is obtained:

$$CTDI_{100}(mAs) = a \times mAs + b \tag{4}$$

Table 1 represents the results as the weighted computer tomography dose index ($CTDI_w$) measured on (mGy) for the abdominal and head phantom volume. Where, columns 1 represents the

energy of the X-ray beam used under 100 (mAs) tube current and 1 sec acquisition time. Columns 2 and 3 show the results for the PMMA abdominal and head volumes, respectively. An excellent agreement can be seen between our results, and that discussed by R. Kramer et al. in the paper [23].

5. Conclusion

In this paper, we have discussed the computed tomography dose index (CTDI) estimation for various diameter organs using PMMA phantom characteristics that were implemented based on the Monte Carlo method. We have therefore modeled all physical aspects of a simple CT scan device. A different energy spectral value of X-ray tube dose was calculated under the SPEKTR3.0 software. It was also integrated into the simulation protocol of dose measurements. After 10^7 particles were generated, measurements of CTDI organs were taken in the head and abdominal phantoms at different parameters such as photon energy (kVp) and tube current (mAs) levels. The results of this study confirmed that the CT dose decreased non-linearly shape as a function of the diameters for various (kVp) and (mAs) values. Also, the CT dose increased non-linearly as a function of the (kVp) values for different (mAs) values but is linearly function increase as function tube current (mAs) values. In the second part, we demonstrated that for the smaller diameters, the absorbed dose (CTDI) increased when the tube current (mAs) is increased and in the different position of the ionization chamber. This result indicates that the average percent absorbed dose received by an abdominal phantom with a diameter equal to 64 cm was lower than 80% of the CTDI value received by the head phantom of 16 cm of diameter, which was slightly higher. Further research simulation for a very high number of particles using GPU code has to be accomplished to decrease the computation time and to obtain a good realistic simulation. Dynamic Bowtie beam CT will also be investigated in that simulation context in the future.

Acknowledgments

The study was performed at the University of Sciences and technology-MB of Oran, Algeria. The authors acknowledge with gratitude the support from the Faculty of Physics. Our sincere thanks go out to all IBN BAJA Supercomputer team.

Conflict of interest

The authors declare no conflict of interest.

Author contributions

M.A. and R.B. conceived of the presented idea and performed the numerical simulations, to the analysis of the results and wrote the manuscript with input from all authors.

References

1. Ghavami SM, Mesbahi A, Pesianian I (2012) Patient doses from X-ray computed tomography examinations by a single array detector unit: Axial versus spiral mode. *Int J Radiat Res* 10: 89–94.
2. Ngaile JE, Msaki PK (2006) Estimation of patient organ doses from CT examinations in Tanzania. *J Appl Clin Med Phys* 7: 80–94.
3. Saravanakumar A, Vaideki K, Govindarajan KN, et al. (2016) Establishment of CT diagnostic reference levels in select procedures in South India. *Int J Radiat Res* 14: 341–347.
4. Kramer R, Cassola VF, Andrade MEA, et al. (2017) Mathematical modelling of scanner-specific bowtie filters for Monte Carlo CT dosimetry. *Phys Med Biol* 62: 781–809.
5. National Research Council (2006) *Health Risks from Exposure to Low Levels of Ionizing Radiation: BEIR VII Phase 2*, Washington DC: The National Academies Press.
6. ICRP, ICRP Publication 103, The 2007 Recommendations of the International Commission on Radiological Protection, 2007. Available from: https://journals.sagepub.com/doi/pdf/10.1177/ANIB_37_2-4.
7. Liu FL, Wang G, Cong WX, et al. (2013) Dynamic bowtie for fan-beam CT. *J X-Ray Sci Technol* 21: 579–590.
8. Williams LE (2003) Therapeutic applications of Monte Carlo calculations in nuclear medicine. *J Nucl Med* 44: 991.
9. Fallah Mohammadi GR, Riyahi Alam N, Geraily G, et al. (2016) Thorax organ dose estimation in computed tomography based on patient CT data using Monte Carlo simulation. *Int J Radiat Res* 14: 313–321.
10. Guidez J, Saturnin A (2017) Evolution of the collective radiation dose of nuclear reactors from the 2nd through to the 3rd generation and 4th generation sodium-cooled fast reactors. *EPJ Nuclear Sci Technol* 3: 32.
11. Vafapour H, Salehi Z (2018) Comparison of incident air kerma (ki) of common digital and analog radiology procedures in kohgiluyeh and boyer-Ahmad province. *Pol J Med Phys Eng* 24: 37–41.
12. Cranley K, Gilmore BJ, Fogarty GWA (1991) *Data for Estimating X-ray Tube Total Filtration*, UK: Institute of Physical Sciences in Medicine.
13. Sahbaee P, Segars W P, Samei E (2014) Patient-based estimation of organ dose for a population of 58 adult patients across 13 protocol categories. *Med Phys* 41: 072104.
14. Birch R, Marshall M (1979) Computation of bremsstrahlung X-ray spectra and comparison with spectra measured with a Ge (Li) detector. *Phys Med Biol* 24: 505–517.
15. Lee CL, Kim HJ, Chung YH, et al. (2009) GATE simulations of CTDI for CT dose. *J Korean Phys Soc* 54: 1702–1708.
16. Poiata A, Focea R, Creanga D (2012) Pathogen germs response to low-dose radiation—medical approach. *EDP Sci* 24: 06005.
17. Comparison of different methods for measuring CT dose profiles with a new dosimetry phantom, 13th International Radiation Protection Association Congress, Glasgow, Scotland, 2012. Available form: http://www.irpa.net/members/P02.156.pdf.
18. Judy PF, Balter S, Bassano D, et al. (1977) *Phantoms for performance evaluation and quality assurance of CT scanners*. USA: American Association of Physicists in Medicine.

19. Panzer W, Shrimpton PC, Jessen K, et al. European guidelines on quality criteria for computed tomography, EU publications, 2000. Available form: https://op.europa.eu/en/publication-detail/-/publication/d229c9e1-a967-49de-b169-59ee68605f1a.
20. Siewerdsen JH, Waese AM, Moseley DJ, et al. (2004) Spektr: A computational tool for X-ray spectral analysis and imaging system optimization. *Med Phys* 31: 3057–3067.
21. Nagel HD (2000) *Radiation Exposure in Computed Tomography: Fundamentals, Influencing Parameters, Dose Assessment, Optimisation, Scanner Data, Terminology*, 2 Eds., Hamburg: Offizin Paul Hartung Druck GmbH & Co. KGD-20020.
22. Hernandez AM, Boone JM (2014) Tungsten anode spectral model using interpolating cubic splines: unfiltered X-ray spectra from 20 kV to 640 kV. *Med Phys* 41: 042101.
23. Khoramian D, Sistani S, Hejazi P (2019) Establishment of diagnostic reference levels arising from common CT examinations in Semnan County, Iran. *Pol J Med Phys Eng* 25: 51–55.

AIMS Press